ELSEVIER

Journal of Non-Crystalline Solids 284 (2001) 217–222

JOURNAL OF NON-CRYSTALLINE SOLIDS

www.elsevier.com/locate/jnoncrysol

Time dependence and energy-transfer mechanisms in Tm^{3+}, Ho^{3+} and Tm^{3+}–Ho^{3+} co-doped alkali niobium tellurite glasses sensitized by Yb^{3+}

L.C. Courrol [a,*], L.V.G. Tarelho [a], L. Gomes [a], N.D. Vieira Jr. [a], F.C. Cassanjes [b], Y. Messaddeq [b], S.J.L. Ribeiro [b]

[a] *Centro de Lasers e Aplicações, IPEN/CNEN–SP, Cidade Universitária, Travessa R400, Zip 05508-900, São Paulo, Brazil*
[b] *Instituto de Química–UNESP, P.O. Box 355, Zip 14801-970 Araraquara, SP, Brazil*

Abstract

Glass samples with the composition (mol%) $80TeO_2$–$10Nb_2O_5$–$5K_2O$–$5Li_2O$, stable against crystallization, were prepared containing Yb^{3+}, Tm^{3+} and Ho^{3+}. The energy transfer and energy back transfer mechanisms in samples containing 5% Yb^{3+}–5% Tm^{3+} and 5% Yb^{3+}–5% Tm^{3+}–0.5% Ho^{3+} were estimated by measuring the absorption and fluorescence spectra together with the time dependence of the Yb^{3+} $^2F_{5/2}$ excited state. A good fit for the luminescence time evolution was obtained with the Yokota–Tanimoto's diffusion-limited model. The up-conversion fluorescence was also studied in 5% Yb–5% Tm, 5% Yb–0.5% Ho and 5% Yb–5% Tm–0.5% Ho tellurite glasses under laser excitation at 975 nm. Strong emission was observed from $^1G_4$ and $^3F_2$ Tm^{3+} energy levels in all samples. The $^5S_2$ Ho^{3+} emission was observed only in $Yb^{3+}Ho^{3+}$ samples being completely quenched in $Yb^{3+}/Tm^{3+}/Tm^{3+}$ samples.

PACS: 42.65; 42.55; 78.20

1. Introduction

The development of high power lasers for some applications like nuclear fusion has indicated that the Yb^{3+}-doped materials, particularly glasses, are the best host materials due to the energy storage properties in the excited state [1]. The tripositive ion has the [Xe] $4f^{13}$ electron configuration with a small number of well spaced 4f states. The probability of energy loss through inter state non-radiative transitions is therefore smaller than the one observed in other rare-earth ions. Moreover materials doped with Yb^{3+} ions are more efficient emitters when pumped by diode lasers without the possibility of excited state absorption [2].

Several different glass matrix containing Yb^{3+} ions are known and Yb^{3+}-doped tellurite samples have attracted much interest mainly because emission properties (emission cross-section and excited state lifetime) are comparable to those observed for well known laser crystals like Yb:YAG and Yb:YAP [3,4].

The Yb^{3+} ion can also be an excellent sensitizer for Tm^{3+} and Ho^{3+} ions when embedded in crystals or glasses [5], improving the efficiency for the

* Corresponding author. Fax: +55-11 816 9315.
E-mail address: lcourrol@net.ipen.br (L.C. Courrol).

0022-3093/01/$ - see front matter
PII: S0022-3093(01)00405-7

Table 1
Rare-earth concentrations in the studied tellurite glasses

Sample	Density (g/cm^3) ± 0.1	Yb (mol%) (ions/$cm^3 \pm 1 \times 10^{19}$)	Tm (mol%) (ions/$cm^3 \pm 1 \times 10^{19}$)	Ho (mol%) (ions/$cm^3 \pm 1 \times 10^{19}$)
TNKL:Tm		–	5	–
TNKL:Ho		–	–	5
TNKL:Yb	5.5	5 (4.2×10^{20})	–	–
TNKL:Yb:Tm:Ho	6.6	5 (4.7×10^{20})	5 (4.8×10^{20})	0.5 (4.9×10^{19})
TNKL:Yb:Tm	5.5	5 (4.2×10^{20})	5 (4.3×10^{20})	–
TNKL:Yb:Ho	5.5	5 (4.2×10^{20})	–	0.5 (4.4×10^{19})

eye-safe 2 μm laser emission assigned to the $^5I_7 \rightarrow {}^5I_8$ Ho^{3+} transition. This kind of solid state lasers has been investigated for various applications including medicine and dentistry, eye-safe laser radar, among others with fluoride glasses being considered the basic host for developing these materials [5]. However, fluoride glasses have smaller emission cross-sections and spontaneous emission probabilities when compared to some oxide glasses.

Alkali niobium tellurite glasses have been studied before by our group [6]. Some glasses well stable against crystallization and displaying good optical properties for some Nd^{3+} containing compositions were studied [6]. In this paper we present the study of these alkali niobium tellurite glasses doped with Yb^{3+} to produce a new Yb laser host material. We also present results on the efficiency of the energy transfer processes between the pairs $Yb^{3+} \rightarrow Tm^{3+}$, $Yb^{3+} \rightarrow Ho^{3+}$ and $Tm^{3+} \rightarrow Ho^{3+}$ ions in these telurite glasses. It will be shown hereafter that the decay rates of donor ions may be described using standard models such as that of Yokota–Tanimoto [7].

2. Experimental methods

Glasses were prepared as described before [6]. Appropriate mixtures of reagent-grade TeO_2, Nb_2O_5, Li_2CO_3 and K_2CO_3 were melted in gold crucibles for 30 min at 830°C in air. The liquids were quenched to room temperature in steel molds and annealed for 30 min at 320°C. Samples with the base compositions (mol%) $80TeO_2$–$10Nb_2O_5$–$5K_2O$–$5Li_2O$ were prepared containing the rare-earth ions with the concentrations shown in Table 1.

Absorption spectra were obtained with a spectrophotometer (Cary 17 D/OLIS). The luminescence spectra in the visible range were obtained with a 1 m monochromator (SPEX) and a photomultiplier (EMI QB9556) after exciting the sample with a Quantel OPO laser pumped by a second harmonic of Nd:YAG laser (pulses of 4 ns at 10 Hz frequency). Emission decay curves were recorded with a digital oscilloscope (TDS 412 Tektronix). Infrared signals were detected by a fast S-1 extended type photomultiplier detector and analyzed using a signal processing box-car averager (PAR 4402).

3. Results

Absorption spectra are shown in Fig. 1. Electronic transitions were assigned by comparison with literature [8] and the assignments are also shown in the figure.

The Yb^{3+} emission spectra were obtained by excitation into the absorption band of Yb^{3+} at 975 nm. The Yb^{3+} emission cross-section at the $^2F_{5/2} \rightarrow {}^2F_{7/2}$ transition was calculated using the fluorescence lineshape and the expression [8]

$$\sigma_{em}(\lambda) = \frac{\lambda^5 \quad I(\lambda)}{8\pi n^2 c \tau_R \int \lambda I(\lambda)\, d\lambda},$$

where τ_R is the radiative lifetime ($\tau_R = 590$ μs) and the refractive index n is equal to 2.09. With these numbers the emission cross-section of Yb^{3+} in these tellurite glass is around 1.1×10^{-20} cm^{-2} in the 980–1010 nm range, as shown in Fig. 2.

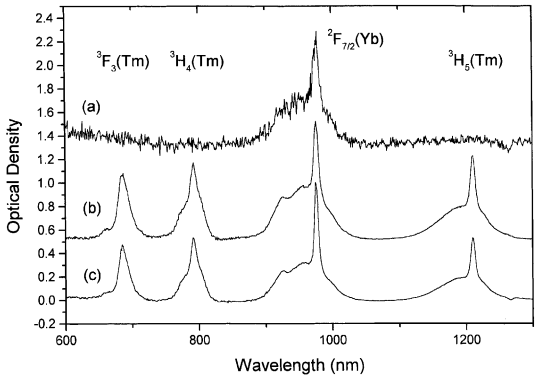

Fig. 1. Absorption spectra for (a) Yb^{3+}, (b) Yb^{3+}/Tm^{3+}, and (c) $Yb^{3+}/Tm^{3+}/Ho^{3+}$ co-doped glasses. Final states for transition arising from the $^3H_6(Tm^{3+})$ and $^2F_{7/2}$ (Yb^{3+}) are indicated.

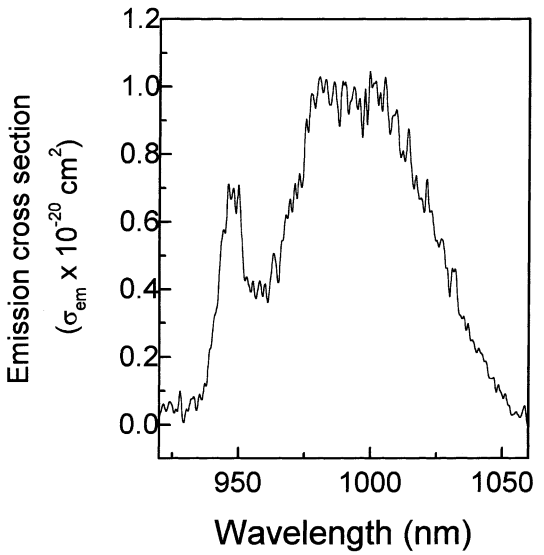

Fig. 2. Emission cross-section for Yb:tellurite glass.

In these tellurite glasses the temporal evolution of the Yb^{3+} $^2F_{5/2}$ level is fit by an exponential function after a short (10 ns) pulse excitation (Fig. 3(a)). The time constant measured is 500 ± 25 μs. The time evolution of the Yb^{3+} fluorescence in co-doped samples has been fitted using the Yokota–Tanimoto expression [7].

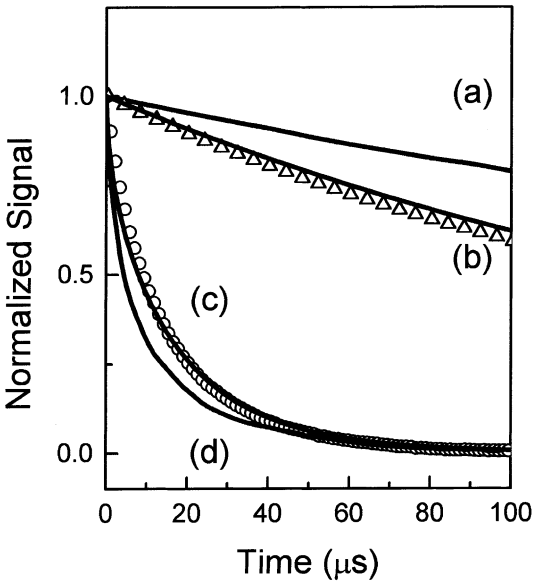

Fig. 3. Yb^{3+} $^4F_{3/2}$ time evolution in niobium alkali tellurite glasses: (a) 5 mol% Yb^{3+}; (b) 5 mol% Yb^{3+} + 5 mol% Tm^{3+}; (c) 5 mol% Yb^{3+} + 0.5 mol% Ho^{3+}; and (d) 5 mol% Yb^{3+} + 5 mol% Tm^{3+} + 0.5 mol% Ho^{3+}. In (b) and (c) the solid lines correspond to Yokota–Tanimoto fits for the decay curves.

$$N(t) = \exp\left[-\frac{t}{\tau} - bt^{1/2}\left(\frac{1+10.87x+15.50x^2}{1+8.743x}\right)^{3/4}\right],$$

$$b = \frac{4}{3}\pi^{3/2} C_A R_0^3 \tau^{-1/2}; \quad x = DR_0^{-2}\tau^{1/3}t^{2/3};$$

$$D = KC_{Yb}^{4/3}.$$

$\tau = 500 \pm 25$ μs is the exponential time-constant of the decay of the Yb^{3+} $^2F_{5/2} \rightarrow {}^2F_{7/2}$ fluorescence obtained in single-doped Yb^{3+} tellurite glass. C_{Yb} and C_A are the Yb^{3+} and Tm^{3+} or Ho^{3+} concentrations. D is the Yb^{3+} diffusion constant due to the excitation energy migration and R_0 represents the critical radius of Yb^{3+}/Tm^{3+} (Yb^{3+}/Ho^{3+}) dipole–dipole interaction. This model considers the effects of diffusion limited energy transfer between rare-earth ions. In this case it is possible to fit the experimental decay curves obtained for donor ions to obtain the diffusion parameters. Table 2 shows the transfer efficiencies obtained from the fit results. From the observation of the Yb^{3+} decay time in Tm^{3+}/Ho^{3+} co-doped samples we obtained the

Table 2
Yb^{3+} diffusion constant (D), critical radius (R_0) of dipole–dipole interactions and energy transfer quantum yields obtained from experimental lifetimes

	R_0 (Å) ± 1	D ($cm^2\ s^{-1}$) ± 10%	η (%) ± 5
Yb/Ho	16	1.12×10^{-13}	43.5
Yb/Tm	10.4	1.08×10^{-10}	96
Yb/Tm/Ho	–	–	95

efficiency for the Tm–Ho energy transfer process (Figs. 3(b)–(d)). The measured lifetime for the Ho^{3+} $^5I_7$ level under 975 nm excitation was estimated to be 2390 ± 25 μs in Yb^{3+}/Ho^{3+} co-doped samples. A decrease to 310 ± 25 μs was observed for the tri-doped ($Yb^{3+}/Tm^{3+}/Ho^{3+}$) sample.

Anti-Stokes emission transitions arising from upper Tm^{3+} levels were also investigated in both Yb^{3+}/Tm^{3+} and $Yb^{3+}/Tm^{3+}/Ho^{3+}$ glasses. In Yb^{3+}/Tm^{3+} glasses emission was observed after Yb^{3+} excitation at 975 nm emission at 480, 650 and 820 nm corresponding to the Tm^{3+} $^1G_4 \rightarrow {}^3H_6$, $^1G_4 \rightarrow {}^3F_4$ and $^3H_4 \rightarrow {}^3H_6$ transitions, respectively as shown in Fig. 4 (note the change in scale for the left and right figures). Ho^{3+} anti-Stokes emission at 540 nm was readily observed in Yb^{3+}/Ho^{3+} co-doped glass and it was not ob-

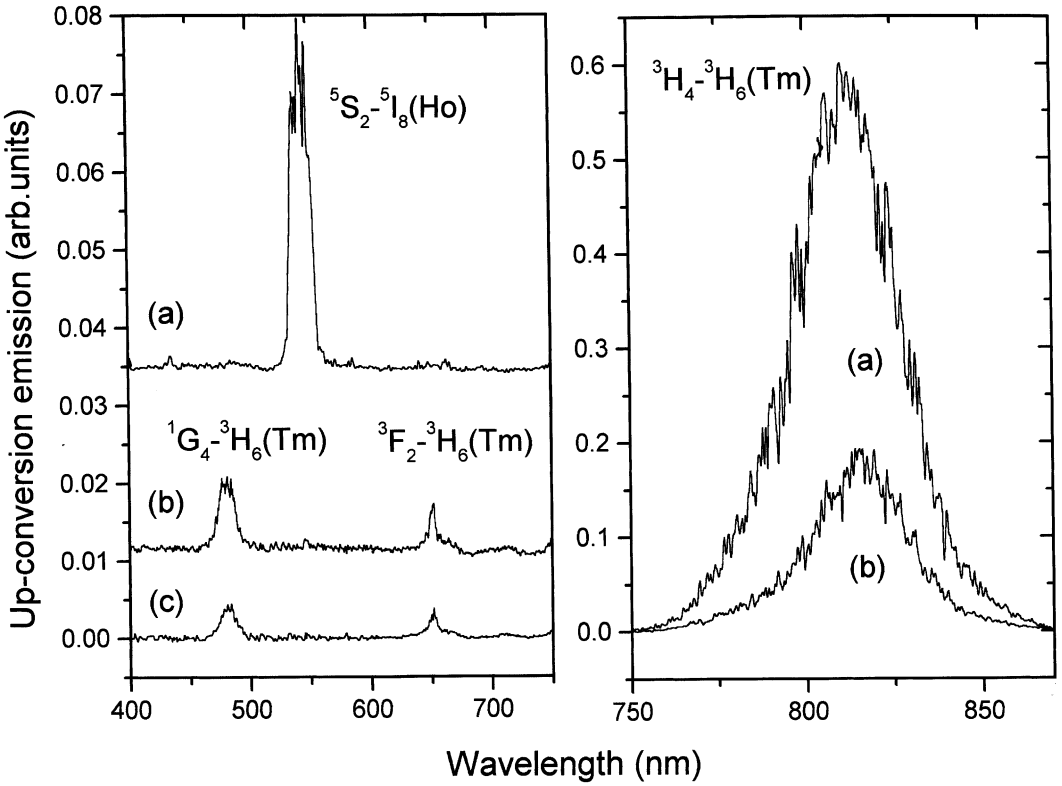

Fig. 4. Left: anti-Stokes emission observed after pumping at 975 nm in (a) Yb^{3+}/Ho^{3+}, (b) Yb^{3+}/Tm^{3+}, and (c) $Yb^{3+}/Tm^{3+}/Ho^{3+}$ co-doped glasses. Right: the same for the 760–860 nm region. (a) Yb^{3+}/Tm^{3+} and (b) $Yb^{3+}/Tm^{3+}/Ho^{3+}$ co-doped glasses. Assignments are indicated in the figure.

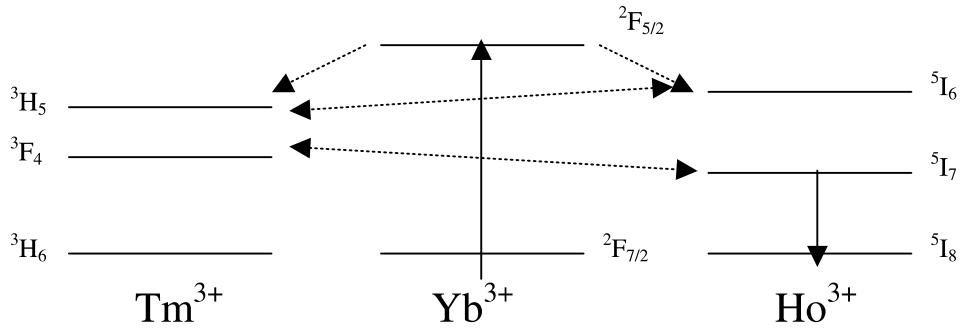

Scheme 1.

served in the $Yb^{3+}/Tm^{3+}/Ho^{3+}$ within the limits of the sensitivity of our detection apparatus.

4. Discussion

The Yb^{3+} emission cross-section (σ_{em}) in niobium alkali tellurite glasses studied here is larger than in other oxide glasses such as silicates, germanates, phosphates and borates [8]. Ligand field effects such asymmetry in the local surrounding of the Yb^{3+} ions and the covalency of the Yb^{3+} first neighbors interaction should account for this larger emission cross-section.

In Yb^{3+}/Tm^{3+}, Yb^{3+}/Ho^{3+} or $Yb^{3+}/Tm^{3+}/Ho^{3+}$ co-doped glasses, the Yb^{3+} emission decay profile is observed to be strongly non-exponential (Fig. 3). $Yb^{3+} \rightarrow Tm^{3+}$ and $Yb^{3+} \rightarrow Ho^{3+}$ energy transfer channels for the Yb^{3+} $^2F_{5/2}$ level should be considered (Scheme 1): Transfer (1): $^2F_{5/2}$ (Yb); $^3H_6$(Tm) $\rightarrow$ $^2F_{7/2}$ (Yb); $^3H_5$ (Tm) and Transfer (2): $^2F_{5/2}$ (Yb); $^5I_8$(Ho) $\rightarrow$ $^2F_{7/2}$ (Yb); $^5I_6$ (Ho). These energy transfer processes are non-resonant as the gap between Yb^{3+} emission and the Tm^{3+} absorption peaks is 1864 cm^{-1}. For the Ho^{3+} absorption peak the gap is 2012 cm^{-1}. Based on these energy values we suggest that in fact a phonon-assisted energy transfer process should apply here.

The Yb^{3+} decay curve in co-doped samples could be fitted by the Yokota–Tanimoto expression [7] since at the Yb^{3+} concentrations used diffusion limited model for the energy transfer between rare-earth ions should apply [8]. The obtained values show that for the $Yb^{3+} \rightarrow Tm^{3+}$ interaction the critical radius is smaller and the diffusion constant is larger than for $Yb^{3+} \rightarrow Ho^{3+}$ interaction. Moreover these times show that the increase of diffusion constant makes the critical radius smaller. We conclude that the energy migration assists the donor–acceptor energy transfer processes. In the systems studied here, the $Yb^{3+} \rightarrow Tm^{3+}$ energy transfer process is more efficient than the $Yb^{3+} \rightarrow Ho^{3+}$ one. The differences in the Tm^{3+} and Ho^{3+} relative concentrations in both samples should account for this observation since this process could be simply related to concentrations of acceptor ions.

Tm^{3+} ($^3H_4 \rightarrow {}^3H_6$) emission overlaps the Ho^{3+} ($^5I_7 \rightarrow {}^5I_8$) absorption band, and two efficient energy transfer channels from Tm^{3+} to Ho^{3+} occur: Transfer (3): $^5I_6$(Ho); $^3H_6$(Tm) $\rightarrow$ $^5I_8$ (Ho); $^3H_5$ (Tm) and Transfer (4): $^4F_4$ (Tm); $^5I_8$ (Ho) $\rightarrow$ $^3H_6$ (Tm); $^5I_7$ (Ho).

We observed however that besides the Ho $\rightarrow$ Tm energy back-transfer, another efficient trap, not identified yet, diminishes the $^5I_7$ level lifetime. The complete understanding of Tm and Ho dynamics is complex, and will be verified in a future work.

5. Conclusions

Emission cross-section of 1.1×10^{-20} cm^2 in the 980–1010 nm range, with fluorescence lifetime of 500 ± 25 μs, were obtained for Yb^{3+}-doped

niobium tellurite glasses, showing that this material can be used in the development of terawatt table top lasers.

The energy transfer from Yb^{3+} to Tm^{3+} is more efficient (96%) than the Yb^{3+} to Ho^{3+} energy transfer (43%). Tm^{3+} and Ho^{3+} anti-stokes emission was also observed. In tri-doped glass sample the Ho^{3+} up-conversion is much smaller due to the resonant $^5I_6$ (Ho) $\rightarrow$ $^3H_5$ (Tm) transfer.

Acknowledgements

Authors acknowledge the Brazilian agencies FAPESP (grants 95/09503-5, 96/07933-5 and 96/01239-0), CNPq and PRONEX for financial support.

References

[1] J. Nies, S. Biswal, F. Druon, J. Faure, M. Nantel, G.A. Mourov, A. Nishimura, H. Takuma, J. Itatani, J.C. Chateloup, C. Hönninger, IEEE J. Selec. Topics Quantum Electron. 4 (2) (1998) 372.
[2] D.P. Bour, D.B. Gilbert, K.B. Fabian, J.P. Bednarz, M. Ettenburg, IEEE Photon. Technol. Lett. 2 (1990) 173.
[3] C. Jiang, F. Gan, J. Zhang, P. Deng, G. Huang, Mater. Lett. 41 (4) (1999) 209.
[4] L.D. Deloach, S.A. Payne, L.L. Chase, L.K. Smith, W.L. Kway, W.F. Krupke, IEEE J. Quantum Electron. 29 (4) (1993) 1179.
[5] Bo Peng, T. Izumitani, Opt. Mater. 4 (1995) 797.
[6] F.C. Cassanjes, Y. Messaddeq, L.F.C. DeOliveira, L.C. Courrol, L. Gomes, S.J.L. Ribeiro, J. Non-Cryst. Solids 247 (1999) 58.
[7] M. Yokota, O. Tanimoto, J. Phys. Soc. Jpn. 22 (1967) 779.
[8] R. Reisfeld, C.K. Jorgensen, in: K.A. Gschneidner, L. Eyring, Handbook on the Physics and Chemistry of Rare Earths, 1987, p. 1 (Chapter 58).